Standalone GPS-Based Flight Inspection System

Euiho Kim, Todd Walter, and J.D. Powell, *Stanford University*

BIOGRAPHY

Euiho Kim is a Ph.D. candidate in the Aeronautics and Astronautics Department at Stanford University. He received his B.S. in Aerospace Engineering in 2001 from Iowa State University and his M.S. from Stanford University in 2002. His research currently focuses on precise positioning using GPS/WAAS and flight inspection systems.

Dr. Todd Walter received his B. S. in physics from Rensselaer Polytechnic Institute and his Ph.D. in 1993 from Stanford University. He is currently a Senior Research Engineer at Stanford University. He is a co-chair of the WAAS Integrity Performance Panel (WIPP) focused on the implementation of WAAS and the development of its later stages. Key contributions include: early prototype development proving the feasibility of WAAS, significant contribution to MOPS design and validation, co-editing of the Institute of Navigation's book of papers about WAAS and its European and Japanese counterparts, and design of ionospheric algorithms for WAAS. He was the co-recipient of the 2001 ION early achievement award.

Prof. J. David Powell received his B.S. degree in Mechanical Engineering from MIT and his Ph.D in Aero/Astro from Stanford in 1970. He joined the Stanford Aero/Astro Department Faculty in 1971 and is currently an Emeritus Professor. Recent focus of research is centered around applications of GPS: applications of the FAA's WAAS for enhanced pilot displays, the use of WAAS and new displays to enable closer spacing on parallel runways, and the use of WAAS for flight inspection for conventional navigation aids. He has co-authored two text books in control systems design.

INTRODUCTION

The Instrument Landing System (ILS) is the current primary landing guidance system worldwide. The Microwave Landing System (MLS) may also become important in the future. Since proper guidance is extremely important, the civil aviation authorities of every country periodically check the ILS coverage, interference, and accuracy, a procedure called Flight Inspection (FI). Among many jobs in flight inspection, it is critical to check whether the ILS provides accurate flight path guidance to a runway during approach. To inspect that in FI, a flight inspection aircraft approaches a runway following the ILS guidance. The flight path during approach is estimated by a Flight Inspection System (FIS) in the aircraft. Then, the estimated flight trajectory is compared with the desired ILS guidance stored in the FIS to see if they match each other within an acceptable tolerance. If there is any deviation in the ILS guidance, a calibration is required. Therefore, a FIS must have the high accuracy in its positioning capability to maintain the accurate guidance of the ILS.

Several flight inspection systems have been used for ILS calibration. Those systems include a theodolite, a laser tracker, and more recently Automated Flight Inspection Systems (AFIS) such as the Inertial-based AFIS and the DGPS-based AFIS [1]. The Inertial-based AFIS is a self-contained system that uses a navigation-grade INS, GPS, a barometric altimeter, a radar altimeter, and a TeleVision Positioning System (TVPS). This system uses the navigation-grade INS coupled with GPS and the barometric altimeter to obtain fine resolution velocity data during approach. The radar altimeter measures the relative distance of an airplane from the ground at the runway threshold and end. The TVPS measures cross-track and along-track offsets from the runway centerline and the threshold marks by using its captured camera images. Since the runway coordinates are accurately surveyed, both of the radar altimeter and the TVPS provide accurate 3D position fixes of the airplane at the runway threshold and end. To estimate flight path during approach, the Inertial-based AFIS integrates the blended velocity backward from the position fix at the threshold. Another position fix at the runway end helps to further refine the blended velocity, thus improving the position solutions. On the other hand, the DGPS-based FIS uses carrier phase differential GPS or RealTime Kinematic (RTK) DGPS. This system provides much better accuracy than the Inertial-based FIS, but it requires of installing a reference receiver on the ground near the runway, which is very time-consuming. Most countries use either one of the systems based on their preferences in terms of accuracy, cost, and efficiency. In the U.S., the FAA prefers to use the Inertial-based AFIS in spite of the high cost mainly caused by the navigation grade INS. The reason is that a Flight Inspection System (FIS) must have a high efficiency and be able to perform fast inspection

procedures to inspect numerous ILS's over the U.S. in a limited time. Other relatively small countries typically choose the DGPS-based AFIS because this system has better accuracy and lower cost.

Previously, from an effort to replace the Inertial-based AFIS to a lower cost system, the WAAS-aided FIS and the WAAS-based FIS were proposed in [2] and [3]. These systems offer better performance than the Inertial-based AFIS in terms of accuracy, efficiency, and cost. However, their operation area is limited to where the WAAS (or any SBAS) is available. In this paper, we introduce the standalone GPS-based FIS that overcomes the shortcomings of the current AFIS's and is operational worldwide. The Standalone GPS-based FIS is a system equipped with a single frequency GPS receiver, a radar altimeter and a TeleVision Positioning System (TVPS). In this system, the flight path is obtained from adding an accurate position fix over the runway threshold to the relative positions obtained from GPS. The reference position is provided from the radar altimeter and the TVPS as the Inertial-based AFIS. A specialized positioning algorithm called "Time-Differenced Precise Relative Positioning (T-D PRP)" generates precise relative positions by using the difference of carrier phase measurements at two epochs. Taking advantage of near real-time positioning allowed in FI, the T-D PRP eliminates differential ionospheric delay errors from the position fix over the threshold to any points during approach. In addition, to ensure the integrity of the position solutions, this system has a specialized RAIM (Receiver Autonomous Integrity Monitoring), or "FIS-RAIM", for FI.

This paper is organized as follows. First, the nature of the ILS calibration problem and its accuracy requirements are introduced. Since the calibration problem of the ILS and the MLS are identical, this paper will only refer to the ILS. Then, the details of the proposed standalone GPS-based FIS are discussed, including its system architecture, the positioning algorithm, the ionospheric delay compensation technique with a single frequency receiver, the satellite exclusion tests, and the FIS-RAIM. Thirdly, the test results from implementing the standalone GPS-based FIS with flight test data are presented. Lastly, conclusions are provided.

ILS CALIBRATION PROBLEM AND FLIGHT INSPECTION SYSTEM ACCURACY REQUIREMENTS

The ILS consists of a glideslope, a localizer and marker beacons. A localizer and a glideslope provide horizontal and vertical guidance to a runway. Marker beacons alert a pilot of his/her approaching specific waypoints with an audible alert. Therefore, the guidance from a glideslope and a localizer is the main objective for the ILS calibration in Flight Inspection (FI).

The ILS calibration problem is unique among other estimation problems. First, the aircraft's trajectory is allowed to be estimated in near real time, i.e., within a few minutes of real time. Secondly, the surveyed runway threshold position can be used to estimate flight paths during approach and indeed is being used in the Inertial-based AFIS. Therefore, a FI procedure using these features, as with the Inertial-based AFIS, can have two modes: approach mode and flight trajectory estimation and ILS calibration mode as illustrated in Figure 1. Thirdly, the duration of the approach mode is usually less than a few minutes. Therefore, only a short set of measurements is available. Lastly, the accuracy required for a Flight Inspection System (FIS) is not rectilinear. Since the ILS is an angular guidance system, the accuracy requirements of a FIS is also angular. The FAA uses the following guidelines: For CAT I ILS, an estimation error should be less than 0.05 deg from glideslope and localizer antennas but not less than 30cm in vertical and 60cm in cross-track. For CAT II•III ILS, an estimation error should be less than 0.015 deg from glideslope and localizer antennas but not less than 30cm in vertical and 60cm in cross-track. In other words, the accuracy requirements become looser as the distance from those antennas increases if XYZ Cartesian coordinates are used. The vertical FIS accuracy requirements for ILS calibration are shown in Figure 2.

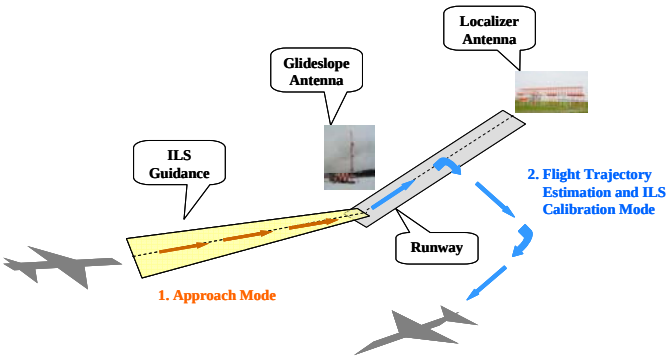

Figure 1: Two Flight Inspection Modes in ILS Calibration

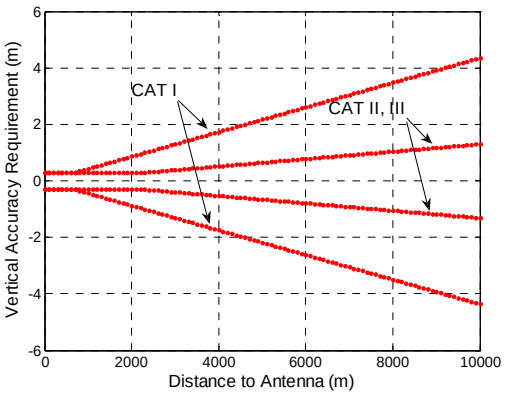

Figure 2: Vertical Accuracy Requirements of Flight Inspection Systems for ILS Calibration

STANDALONE GPS-BASED FLIGHT INSPECTION SYSTEM

This section discusses the details of the standalone GPS-based Flight Inspection System (FIS). The overall architecture, its specific positioning algorithms, and the FIS-RAIM are presented.

a. System Architecture

The standalone GPS-based FIS has a single frequency GPS receiver, a radar altimeter and a TVPS (TeleVision Positioning System). The same kinds of radar altimeter and TVPS being used in the current Inertial-based AFIS are taken in the standalone GPS-based FIS. The 95% accuracy of the radar altimeter is better than 15cm [4]. The 95% accuracy of the TVPS is better than 15cm in cross-track and 30cm in along-track [5]. This integrated system is optimally designed for the ILS calibration problem in terms of accuracy, cost, and efficiency.

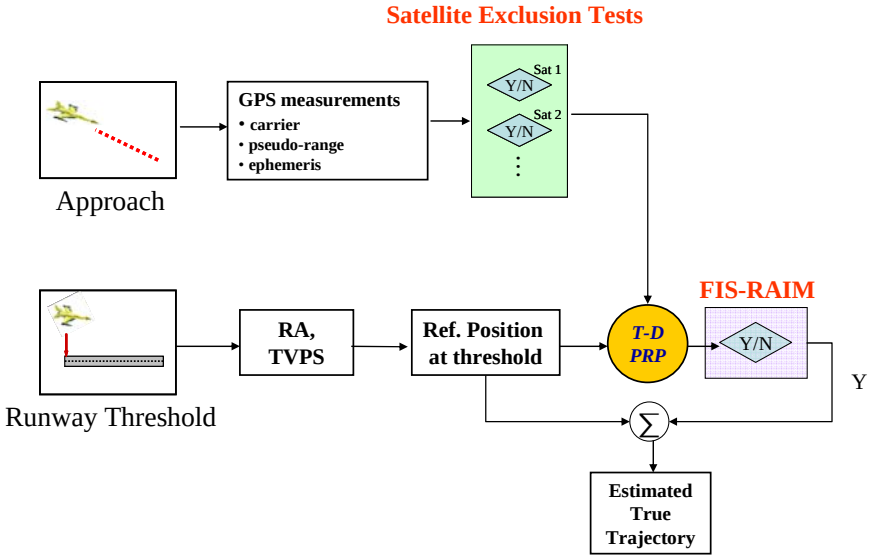

Figure 3: System Architecture of the Standalone GPS-Based FIS

Figure 3 illustrates the overall algorithm of the standalone GPS-based FIS. During approach, GPS measurements are collected. Over the threshold of a runway, the radar altimeter measures the vertical distance between the airplane and the runway threshold. At that point, the TVPS measures the cross-track and along-track deviations of the airplane from the center line and the threshold mark of the runway by using its camera images. Since the position of the threshold is accurately surveyed, the radar altimeter and the TVPS provide an accurate instant 3D position of the airplane over the threshold. A specialized positioning algorithm, Time-Differenced Precise Relative Positioning (T-D PRP) method, uses this

reference position and the carrier phase measurements to compute precise relative positions. The estimated flight path during approach is obtained by adding the relative positions to the reference position. The detailed algorithm of the T-D PRP will be discussed in the next subsection. To ensure sound position solutions, satellite exclusion tests are implemented to discard a satellite that should not be used in T-D PRP. In addition, the integrity of the T-D PRP solutions is checked in the FIS-RAIM that protects against possible satellite failures.

b. Time-Differenced Precise Relative Positioning (T-D PRP)

The Time-Differenced precise relative positioning (T-D PRP) was introduced in [3]. In summary, the T-D PRP uses the difference of carrier phase measurements at two epochs as ranging sources. Since standalone GPS is only available in this system, satellite clock error corrections are based on the GPS navigation messages. Tropospheric errors are compensated by using the same model that the WAAS uses [6]. The differential ionospheric delay errors at the two epochs are removed by using code minus carrier phase measurements.

The GPS carrier phase measurements have the following expression.

$$\Phi = r + c[\delta t_u - \delta t_s] - I + T + N + \varepsilon \tag{1}$$

where r is the true range between a receiver and a satellite, c is the speed of light, and δt_u and δt_s are receiver and satellite clock errors, respectively. I is an ionospheric delay in L1 frequency and T is a tropospheric delay. N is an integer ambiguity. ε includes multipath, thermal noises, and modeling errors in carrier phase measurements.

Assuming that there is no cycle-slip, a single difference of carrier phase measurements from a satellite k at two epochs, t and 0, is as follows.

$$\Phi_t^k - \Phi_0^k = r_t^k - r_0^k + c\Delta t_u - c\Delta t_s^k - \Delta I_t^k + \Delta T_t^k + \Delta \varepsilon_t^k \tag{2}$$

where $\Delta(\bullet)$ is the difference of the same variable at the two epochs.

Now, let us apply satellite clock error corrections and tropospheric error corrections to Equation (2). Then, linearizing it with respect to a reference position, Equation (2) becomes with a short base line assumption

$$\begin{aligned} y_{t,0}^k &= r_t^k - r_0^k - (\hat{r}_{R,t}^k - \hat{r}_{R,0}^k) + c\Delta t_u - \Delta I_t^k + \Delta \tilde{\varepsilon}_t^k \\ &= -1_t^k \bullet \delta x_{t,0} + c\Delta t_u + b_{\mathrm{Ref},t}^k - \Delta I_t^k + \Delta \tilde{\varepsilon}_t^k \end{aligned} \tag{3}$$

where $\hat{r}_R^k$ is the computed distance between the satellite k and a reference position using the broadcast ephemeris. 1_t^k is a line of sight vector to the satellite k at time t. $\delta x_{t,0}$ is a relative position of a receiver at time t from the position at time 0. $b_{\mathrm{Ref},t}$ is an error caused from the imperfect knowledge of reference position at time t. $\Delta \tilde{\varepsilon}_t^k$ includes residual correction errors and higher order modeling errors due to the linearization in addition to $\Delta \varepsilon_t^k$. Since $c\Delta t_u$ is common to the all satellites, it should be easily estimated. Therefore, the error sources in Equation (3) are $b_{\mathrm{Ref},t}$, ΔI, and $\Delta \tilde{\varepsilon}$.

$\Delta \tilde{\varepsilon}$ includes tropospheric delay correction residuals, satellite clock correction residuals, multipath, modeling errors, thermal noise and so on. $\Delta \tilde{\varepsilon}$ is also very small when t is near to zero and increases as t increases because the residual correction errors are highly correlated [7, 8]. Fortunately, multipath and other receiver related noise are small (~1 or 2cm) enough for our application so that they are not of our concern.

Now, let us assume that we know satellite locations perfectly to see the sole effects of reference position errors. When the exact reference position is known, $b_{\mathrm{Ref},t}$ is zero. However, when the reference position has some errors, the computed distance between the satellite k and a reference position has the following expression.

$$\hat{r}_{R,t}^k = r_{R,t}^k - 1_t^k \bullet \delta x_{\mathrm{bias}} \tag{4}$$

where δx_{bias} is a reference position error vector pointing from true position. Then,

$$\begin{aligned} r_t^k - \hat{r}_{R,t}^k &\approx -1_t^k \bullet \delta x_{t,0} + 1_t^k \bullet \delta x_{\text{bias}} \\ -r_0^k + \hat{r}_{R,0}^k &\approx -1_0^k \bullet \delta x_{\text{bias}} \end{aligned} \tag{5}$$

Therefore, $b_{\text{Ref},t}^k$ is

$$b_{\text{Ref},t}^k \approx 1_t^k \bullet \delta x_{\text{bias}} - 1_0^k \bullet \delta x_{\text{bias}} \tag{6}$$

From (6), we can see that $b_{\text{Ref},t}^k$ is small when *t* is near to zero and increases as *t* increases.

Next, ΔI is removed by using the difference of L1 code and carrier phase measurements, assuming that ΔI behaves linearly during approach. The correction for ΔI will be very effective in where ionosphere is active and minimal in where ionosphere is steady. However, even in the regions that have quiet ionosphere, the correction for ΔI is indispensable because it is always possible that an unexpected sharp ionospheric gradient may arise. More details of the estimation of ΔI will be discussed in the next subsection.

Finally, a set of linear equations can be formed as follows.

$$\underbrace{\begin{bmatrix} y_{t,0}^1 \\ y_{t,0}^2 \\ \vdots \\ y_{t,0}^n \end{bmatrix}}_{Y} = \underbrace{\begin{bmatrix} -1_t^1 \; 1 \\ -1_t^2 \; 1 \\ \vdots \\ -1_t^k \; 1 \end{bmatrix}}_{G} \underbrace{\begin{bmatrix} \delta x_{t,0} \\ C\Delta t_u \end{bmatrix}}_{X} + \underbrace{\begin{bmatrix} \hat{\varepsilon}_t^1 \\ \hat{\varepsilon}_t^2 \\ \vdots \\ \hat{\varepsilon}_t^k \end{bmatrix}}_{\hat{\varepsilon}} \tag{7}$$

$$Y = GX + \hat{\varepsilon}$$

where $\hat{\varepsilon}$ includes $b_{\text{Ref},t}$, $\Delta\tilde{\varepsilon}_t$, and residual errors from the compensation of ΔI.

Then, the relative position from T-D PRP with respect to the reference position is computed using weighted least squares as follows

$$X = (G^T W^{-1} G)^{-1} G^T W^{-1} Y \tag{8}$$

where *W* is a weighting matrix. It is difficult to find an optimal *W* because some of the errors in *Y* are highly correlated over time. However, since the overall errors have dependency on a satellite elevation angle, a reasonable choice for its elements would be as a function of the satellite elevation angle.

Overall, the error characteristic of the T-D PRP is that the error is very small when *t* is near to zero and grows over time. This error characteristic is well suited for the ILS calibration problem as long as it is kept low enough not to violate the ILS calibration accuracy requirement.

c. Ionospheric Delay Gradient Estimation using Linear Regression with a Single Frequency Receiver

This subsection briefly introduces the ionospheric delay gradient estimation with a single frequency receiver [9]. The estimated ionospheric delay gradient is used to make a correction for the differential ionospheric delays between a reference position and during approach.

The code phase measurements, ρ, from a GPS receiver can be written as

$$\rho = r + c[\delta t_u - \delta t_s] + I + T + M \tag{9}$$

where M includes multipath, thermal noises, and modeling errors in the code phase measurement

The code minus carrier phase measurement at time t is

$$\rho_t - \Phi_t = 2I_t - N + M_t - \varepsilon_t \tag{10}$$

This difference includes ionospheric delays, an integer ambiguity and noise in code and carrier phase measurements. Our interest, here, is to estimate a slant ionospheric delay gradient. It should be noted that the ionospheric delays slowly change with respect to time during nominal ionospheric days. Therefore, the gradient can be assumed as a constant during a short time window (tens of minutes). Assuming a constant ionospheric delay gradient, Equation (10) can be rewritten as

$$\begin{aligned} \rho_t - \Phi_t &= \beta_0 + 2t \cdot \beta_1 + M_t - \varepsilon_t \\ &\approx \beta_0 + 2t \cdot \beta_1 + M_t \end{aligned} \tag{11}$$

In Equation (11), ε_t is ignored because it is much smaller than M_t.

Expressing the time series of equation (11) in a matrix form yields

$$\underbrace{\begin{bmatrix} \rho_{t_0} - \Phi_{t_0} \\ \rho_{t_1} - \Phi_{t_1} \\ \vdots \\ \rho_{t_n} - \Phi_{t_n} \end{bmatrix}}_{\Gamma} = \underbrace{\begin{bmatrix} 1 & 2 \cdot t_0 \\ 1 & 2 \cdot t_1 \\ & \vdots \\ 1 & 2 \cdot t_n \end{bmatrix}}_{\Psi} \underbrace{\begin{bmatrix} \beta_0 \\ \beta_1 \end{bmatrix}}_{\beta} + \underbrace{\begin{bmatrix} M_{t_0} \\ M_{t_1} \\ \vdots \\ M_{t_n} \end{bmatrix}}_{\Omega} \tag{12}$$

$$\Gamma = \Psi\beta + \Omega$$

Now, the problem becomes to find β in the presence of Ω. If Ω is white nose, the ordinary least-squares (OLS) is the best estimator. Fortunately, airborne multipath is very close to white noise [9]. Therefore,

$$\hat{\beta}_{OLS} = (\Psi^T \Psi)^{-1} \Psi^T \Gamma \tag{13}$$

Once we have the estimated ionospheric delay gradient, $\hat{\beta}_1$, the differential ionospheric delay correction between a reference position and during approach is simply

$$\Delta\hat{I}_{t,0} = t \bullet \hat{\beta}_1 \tag{14}$$

It is interesting to see how much the estimated ionospheric delay gradient is useful even during ionospheric nominal days. Figure 4 compares relative positions from implementing the T-D PRP with and without compensating for the differential ionospheric delays using static experimental receiver data. The error growth was significantly reduced when the differential ionospheric delays were compensated.

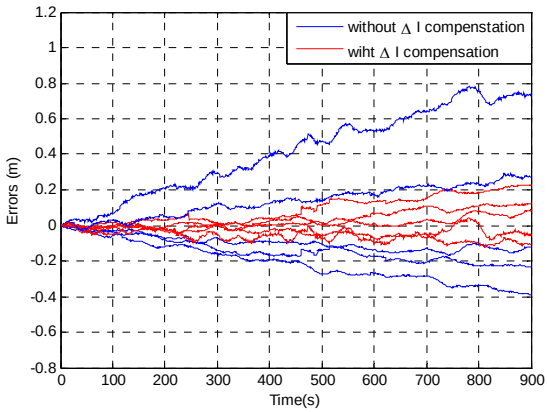

Figure 4: Example of the Effectiveness in Applying $\Delta\hat{I}$. The measurements were Taken on Sept/05/2005 at Stanford University.

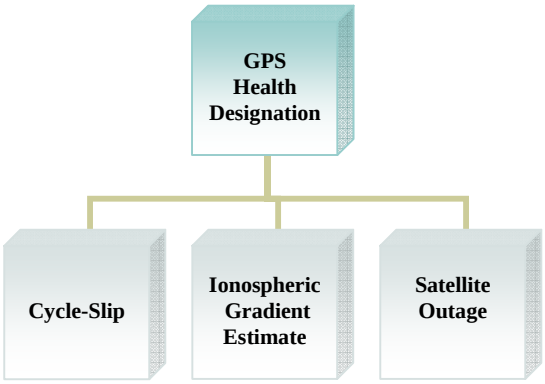

Figure 5: A chart of Lists for Satellite Exclusion Criteria.

d. Satellite Exclusion Tests

Figure 5 shows a chart of the lists that should be checked before including a satellite in the T-D PRP. The first check is to see if there are any satellites designated as UNHEALTH in the navigation messages. Any satellite experiencing a cycle-slip during approach is also excluded because the T-D PRP must use continuously accumulated carrier phase measurements. In addition, the goodness of fit for the estimation of ionospheric delay gradient must be examined. Any ionospheric delay gradients showing a severe nonlinear behavior can be detected by analyzing the residuals after fitting a first order linear model on code minus carrier phase measurements. Chi-square tests are a good indicator for goodness of fit [10]. Lastly, it is best to use the same set of satellites that are fully available during the entire approach. A different set of satellites may introduce a sudden jump in relative positions, which is very undesirable for our application.

e. RAIM in Flight Inspection (FIS-RAIM)

A RAIM (Receiver Autonomous Integrity Monitoring) is commonly used as an integrity monitor to detect a satellite failure and isolate and exclude the faulty satellite when there is no integrity information available from an augmentation system such as SBAS (Space-Based Augmentation System). Also, when the satellite geometry is too poor to detect a satellite failure, a RAIM issues an alarm to indicate that integrity can't be assured. For the same reason, the standalone GPS-based FIS must have an integrity monitor. However, due to the different positioning algorithm and operational requirements in the standalone GPS-based FIS, the pre-installed standard RAIM [11] in a GPS receiver may not be suited for this system. One of the reasons is that the standard RAIM is designed to protect against a large satellite failure, but the standalone GPS-based FIS needs to be protected against even a slow ramp clock error (for example, even one centimeter per second) that is not typically detected as a satellite failure in the standard RAIM. Nonetheless, the principle of the conventional RAIM method can be exactly adapted to this system. Among various RAIM methods, the standalone GPS-based FIS uses the maximum separation of solutions [12]. This subsection only discusses a satellite failure detection using the FIS-RAIM.

When minor satellite failures occur, such as a slow ramp satellite (a few cm/s) clock error or a low amplitude (less than a few meters) satellite dithering, the standard RAIM may not detect them until those errors are significantly developed to cause position errors more than tens of meters. However, since the accuracy requirements in Flight Inspection (FI) are very tight, even those minor satellite failures may cause critical positioning failures in the standalone GPS-based FIS. Figure 6 shows two examples of positioning failures in vertical when one of the satellites has a 4cm/s ramp clock error and a sinusoidal clock dithering with 1 meter amplitude during approach. These results are obtained from a real flight test data with simulated satellite failures.

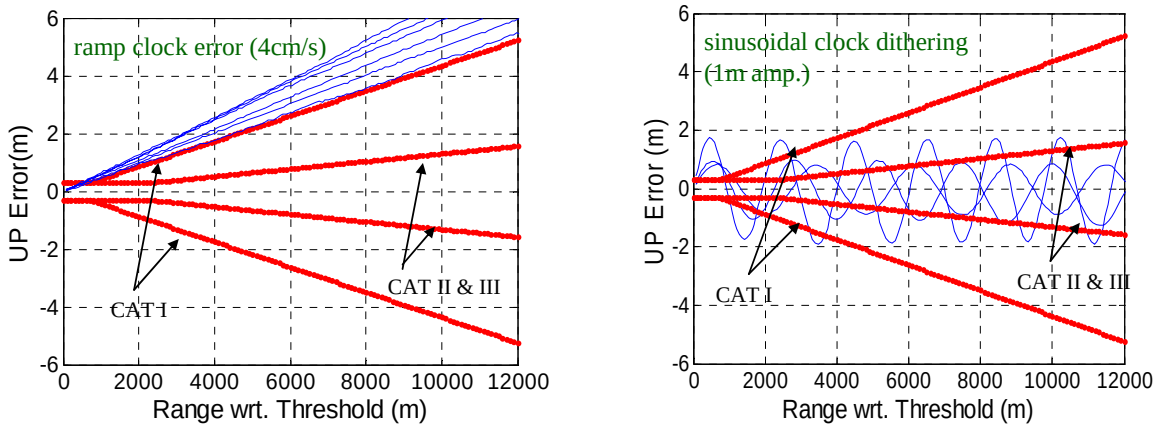

Figure 6: Positioning Failures of the T-D PRP in Vertical with Simulated a 4cm/s Ramp Satellite Clock Error and 1Meter Amplitude Sinusoidal Clock Dithering during Approach. The Two Red lines are Accuracy Requirements.

To protect against the minor satellite failures, the FIS-RAIM, a RAIM in the standalone GPS-based FIS, uses the maximum separation of solutions [12]. The principle of the maximum separation of solutions is as follows. Assuming there is only one possible satellite failure, the method uses the *n* subsets having *n-1* satellites of the *n* satellites in view to check integrity. If the position solutions of the *n* subsets are consistent, there is no satellite failure. If not, an alert is issued. The test statistic used in this method is the maximum observed absolute position difference of the subsets, and a threshold for the test statistic is the preset maximum solution separation under a normal condition. Figure 7 shows the maximum observed absolute position differences of the T-D PRP in vertical for the three cases: no satellite failure, a satellite clock ramp error, and a low amplitude satellite clock dithering.

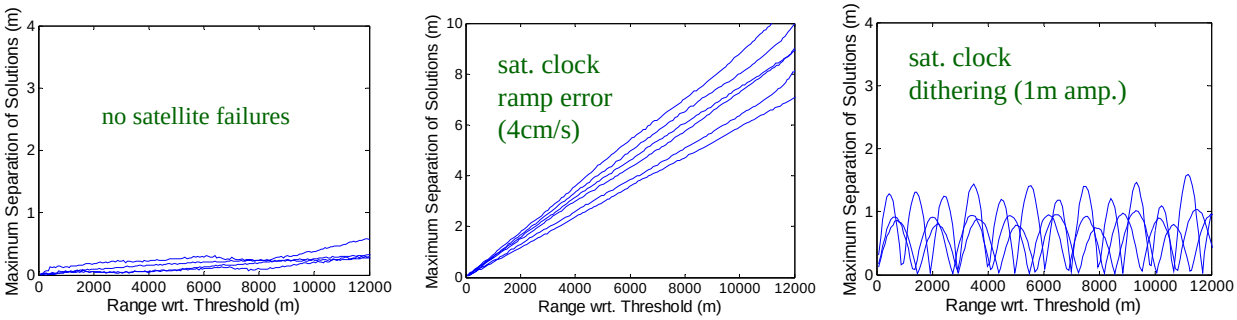

Figure 7: Examples of Observed Maximum Separated Solutions in Vertical during the Approaches Taken on Oct 30, 2006 for the Three Cases; No Satellite Failures, a Ramp Satellite Clock Error, and a Low Amplitude Satellite Clock Dithering

Now, the problem comes to what statistic should be used to differentiate the minor satellite failures from no satellite failures in FI. The statistic and its associated threshold must perform well with the two clock failure examples as well as any arbitrary types of satellite failures. In addition, they must comply with the accuracy requirements so that they do not often give a false alarm when the position solutions have unusually large errors but are still within the requirements. To meet those constraints, the FIS-RAIM utilizes 2 statistics: a slope from fitting the maximum observed separated solutions to a straight line using linear regression and the residual tests on the fitted line. The slope detects any failures having a ramp clock error, and the residual tests identify any failures having a significant clock dithering. Any satellite failures fell between the two cases are more likely detected by either one of them. The threshold for the slope can be chosen by considering both the observed slope during no satellite failure and the accuracy requirements, and the threshold for the residual tests can be determined from the statistics of the residuals under no failure condition.

Figure 8 shows the observed maximum separated solutions during the flight tests of 30 approaches and the residuals from the linear fit. No particular satellite failure was observed during the test. In the left figure, the threshold is set to 0.05/2 deg slope that is the one side of the FIS accuracy requirement for CAT I ILS calibration. When the sum of square of the residuals is used for the residual test, the possible threshold is $(30\text{cm})^2 \times \text{chi2inv}(95\%, n\text{-}2)$, where n is the number of data

used in the regression. These thresholds are conservatively chosen to compensate for the relatively small data set and to minimize false alarms.

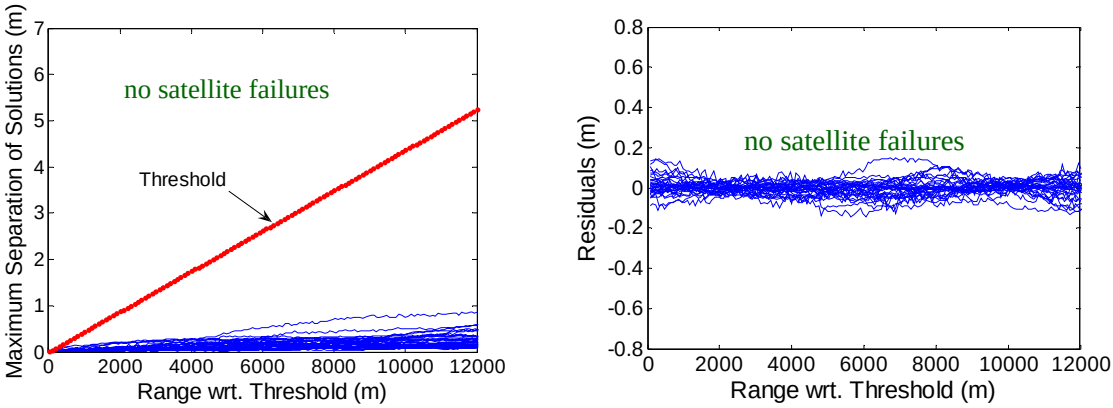

Figure 8: The Left Figure Shows the Observed Maximum Separated Solutions in Vertical during 30 Approaches Taken During Oct 30~31, 2006. The Right Figure Shows the Corresponding Residuals from the Fitted Line of the Separated Solutions in the Left Figure. There Was No Satellite Failure in the Flight Tests.

RESULTS

The standalone GPS-based FIS algorithm was tested with flight test data taken during Oct 30~31, 2006 in collaboration with the FAA AVN at Oklahoma City. During the flight test, DGPS positions from a RTK system were also collected in addition to GPS measurements. The DGPS positions were used as a truth source for the validation of the Standalone GPS-Based FIS. A radar altimeter and a TVPS were not used because there were some hardware difficulties during the tests. Figure 9 shows an example of flight paths during the flight tests in ENU coordinates. The total number of approaches used in this test is 23.

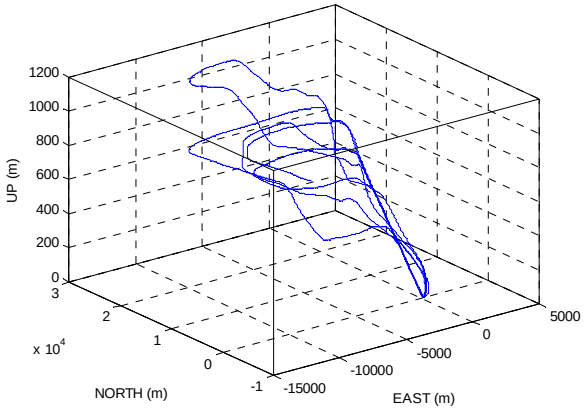

Figure 9: Some of the Flight Trajectories in Flight Tests Taken During Oct 30~31, 2006

a. T-D PRP Tests

Figure 10 shows the horizontal and vertical errors from implementing the T-D PRP. A reference position was given from a DGPS position instead of a radar altimeter and a TVPS at the threshold. The two red lines are FIS accuracy requirements for CAT I and CAT II•III ILS calibration.

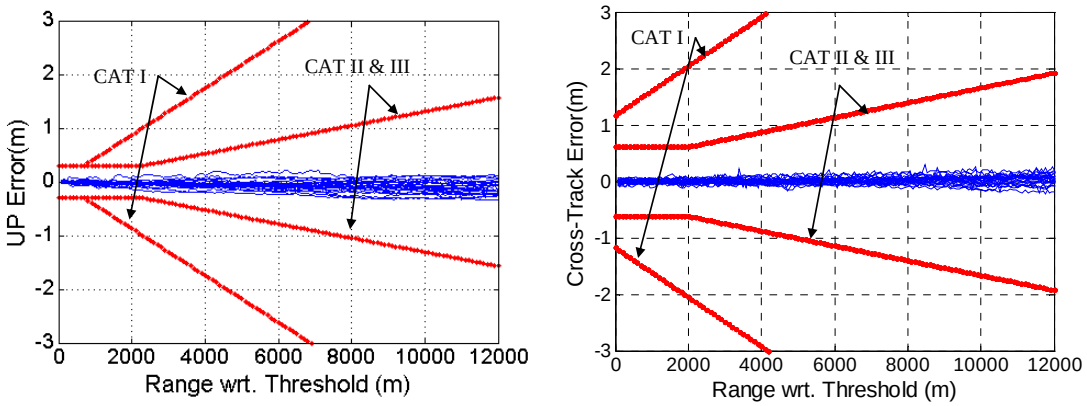

Figure 10: The Vertical and Cross-Track Errors of 23 Approaches from the Standalone GPS-based FIS (without RA and TVPS Errors)

Figure 10 does not represent the total errors of the standalone GPS-based FIS because the reference position errors are not included. However, these results clearly show the error characteristics of the T-D PRP. Based on that, it is possible to measure the performance of the standalone GPS-based FIS using 95% accuracies of the radar altimeter and the TVPS. The total errors will be further discussed in the next subsection.

b. Standalone GPS-Based FIS Performance

Considering the errors from the T-D PRP and the accuracy requirements, the most critical regions are around 2200 meters and 2000 meters from the threshold in vertical and horizontal respectively. To see the performance of the standalone GPS-based FIS, we should consider the total errors caused by both the T-D PRP and the reference position error in cross-track and vertical at the critical regions because those errors may most likely violate the FIS accuracy requirements for CAT II•III ILS calibration. Table 1 summarizes the statistics of the errors from the T-D PRP at the critical regions.

Table 1: Statistics of the T-D PRP Errors at Critical Regions

	Up (m)	Cross-Track (m)
Mean	-0.0345	-0.0013
Std	0.050	0.041
RMS	0.061	0.041

Treating the T-D PRP errors and the reference position errors as zero-mean independent random variables, which is not exactly true but practically good enough, the distributions of the total errors can be easily calculated. Taking the accuracies (95%) of the radar altimeter and the TVPS in the standalone GPS-based FIS to be about 15cm, the total errors at the critical regions have 9.01cm standard deviation in vertical and 8.54cm standard deviation in cross-track. Therefore, the 95% accuracy of the standalone GPS-based FIS is about 18.02cm meters in vertical and 17.10cm in cross-track at the critical regions. Therefore, the standalone GPS-based FIS sufficiently meets the FIS accuracy requirements for CAT II•III ILS calibration whose limits are about 30cm in vertical and 60 cm in cross-track.

CONCLUSION

The standalone GPS-based FIS is introduced in this paper. Its system architecture, positioning algorithm and integrity features are discussed in detail. For the validation of the standalone GPS-based FIS positioning algorithm, this system was tested with flight test data taken during Oct 30~31, 2007 at Oklahoma City. The results meet the FI performance requirements.

The GPS-based FIS provides more optimized performance than the current FIS's in terms of accuracy, cost, and efficiency. Its accuracy is between the Inertial-based AFIS and the DGPS-based AFIS, and its cost is significantly lower than the two AFIS's. The efficiency of the standalone GPS-based FIS outperforms the two AFIS's because it does not need a reference station on the ground nor does it require the FI aircraft to fly level over the whole runway. Compared to the proposed FIS's using the WAAS (SBAS), the WAAS-aided FIS and the WAAS-based FIS have better integrity features because they can

take advantage of the broadcast integrity messages. However, the probability of a satellite failure during FI is expected to be extremely small because a FI is only operated a few days a week and during day time. So, a satellite failure will rarely occur in FI. It is also expected that the FIS-RAIM detects most satellite failures that can cause positioning failures. Overall, the standalone GPS-based FIS is a good alternate where WAAS (SBAS) is not available and provides better performance than the current AFIS's.

ACKNOWLEDGMENTS

The authors gratefully acknowledge the support of FAA flight inspection division (AVN)

REFERENCES

[1] *Flight Inspection History*, International Committee for Airspace Standards and Calibration (ICASC), Available : http://avnwww.jccbi.gov/icasc/fi_history.html

[2] E. Kim, T. Walter, and J.D. Powell, "*A Development of WAAS-Aided Flight Inspection System*", In Proc. IEEE/ION PLANS 2006, San Diego, Apr 24-27, 2006

[3] E. Kim, T. Walter, and J.D. Powell, "*WAAS-Based Flight Inspection System*", In Proc. ION AM 2007, Cambridge, Apr 23-25, 2006

[4] U. Peled, "*Radar Altimeter Evaluation-Refined Runway Data*", internal report, Stanford, California, May 28, 2005

[5] Television Positioning System, NXT. Flight Inspection Systems, Available: http://www.nxt-afis.com/television_positioning_system.html

[6] *Minimum Operational Performance Standards for Global Positioning System/Wide Area Augmentation System Airborne Equipment.* Washington, D.C, RTCA SC-159, WG-2, DO-229C, 28 Nov, 2001.

[7] T. Walter, A. Hansen, and P. Enge, "*Validation of the WAAS MOPS Integrity Equation*", In Proc. ION Annual Meeting 1999, Cambridge, June 28-30, 1999

[8] H.E. Ibrahim and A. El-Rabbany, "*Stochastic Modeling of Residual Tropospheric Delay*", In Proc. ION NTM 2007, San Diego, Jan 22-24, 2007

[9] E. Kim, T. Walter, and J.D. Powell, "*Adaptive Carrier Smoothing using Code and Carrier Divergence*", In Proc. ION NTM 2007, San Diego, Jan 22-24, 2007

[10] Yaakov Bar-Shalom et al., "*Estimation with Application to Tracking and Navigation*" ,New York, Wiely-InterScience, 2001

[11] Brown, R. G., "*A Baseline RAIM Scheme and a Note on the Equivalence of Three RAIM Methods*", NAVIGATION, Journal of The Institute of Navigation, Vol. 39, No. 3, Fall 1992.

[12] Brown, R. G., and McBurney, P. W., "*Self-Contained GPS Integrity Check Using Maximum Solution Separation as the Test Statistic*", In Proc. ION Satellite Division First Technical Meeting 1987, Colorado Springs, 1987